

1     **Subnuclear localisation is associated with gene activation not repression or**  
2                     **parental origin at the imprinted *Dlk1-Dio3* locus**

3  
4     Rahia Mashoodh<sup>1+</sup>, Lisa C. Hülsmann<sup>2+</sup>, Frances L. Dearden<sup>2</sup>, Nozomi Takahashi<sup>2</sup>, Anne C.  
5     Ferguson-Smith<sup>2\*</sup>

6  
7  
8  
9     <sup>1</sup> Department of Zoology, University of Cambridge, Cambridge, United Kingdom

10    <sup>2</sup> Department of Genetics, University of Cambridge, Cambridge, United Kingdom

11

12

13

14

15

16

17

18    \* Corresponding author

19    <sup>+</sup> These authors contributed equally to the work

20    Emails: [afsmith@gen.cam.ac.uk](mailto:afsmith@gen.cam.ac.uk) (ACFS)

21

## 22 **Abstract**

23

24 At interphase, de-condensed chromosomes have a non-random three-dimensional architecture  
25 within the nucleus, however, little is known about the extent to which nuclear organisation  
26 might influence expression or *vice versa*. Here, using imprinting as a model, we use 3D  
27 RNA- and DNA-fluorescence-in-situ-hybridisation in normal and mutant mouse embryonic  
28 stem cells to assess the relationship between imprinting control, gene expression and allelic  
29 distance from the nuclear periphery. We compared the two parentally inherited imprinted  
30 domains at the *Dlk1-Dio3* domain and find a small but reproducible trend for the maternally  
31 inherited domain to be further away from the periphery if the maternally expressed gene  
32 *Gtl2/Meg3* is active compared to when it is silenced. Using *Zfp57*KO ES cells, which harbour  
33 a paternal to maternal epigenotype switch, we observe active alleles significantly further  
34 away from the nuclear periphery with the distance from the periphery being proportional to  
35 the number of alleles active within the cell. This distribution of alleles suggests an activating  
36 effect of the nuclear interior rather than a repressive association with the nuclear periphery.  
37 Although we see a trend for the paternally inherited copy of the locus to be closer to the  
38 nuclear periphery, this appears to be linked to stochastic gene expression differences rather  
39 than parental origin. Our results suggest that transcriptional activity, rather than  
40 transcriptional repression or parental origin, defines sub-nuclear localisation at an  
41 endogenous imprinted domain.

42

## 43 **Author summary**

44

45 Genomic imprinting is an epigenetically regulated process that results in the preferential  
46 expression of a subset of developmentally regulated genes from maternally or paternally  
47 inherited chromosomes. We have used imprinted genes as a model system to investigate the  
48 relationship between the localisation of genes within the cell nucleus and their active  
49 expression while at the same time distinguishing gene repression by genomic imprinting, and  
50 gene repression by other mechanisms that act on the active allele. We find that there is a  
51 significant correlation between transcription and distance to the edge of the nucleus for the  
52 *Gtl2/Meg3* gene in the imprinted *Dlk1-Dio3* region. However, this correlation has a very  
53 small effect size and the nuclear envelope, which is commonly thought to act as a repressive  
54 environment for gene expression, does not appear to play a major role. We show that position  
55 effects, which have been shown for artificially lamina-targeted genes, also exist for  
56 endogenous loci and consider the possible biological relevance of the observed small effect.

57

## 58 Introduction

59

60 The spatial organization of chromosomes in the interphase nucleus is non-random and  
61 involves 3D interactions on chromatin as well as interactions with various nuclear domains,  
62 the nuclear envelope being the best characterized (1). While the bulk of chromosomes is  
63 arranged as relatively compact and spatially defined chromosome territories (2), open  
64 chromatin between these contains transcription factories where active genes from different  
65 genomic loci co-localize at times of transcription (3). Recently, there has been much interest  
66 in understanding ways in which the 3D localisation of chromatin can influence or be  
67 influenced by gene expression (4,5). While chromatin organization into chromosome  
68 territories, topologically associated domains, and loops have complex effects on  
69 transcriptional regulation, interactions with the nuclear envelope are generally seen as  
70 transcriptionally repressive (1). Lamina associated domains (LADs) have been characterized  
71 as gene poor, transcriptionally inactive regions (6), even though these repressed regions have  
72 been shown to be dynamic in dividing cells and are therefore not always lamina-associated in  
73 every cell within a population (7). A notable exception to the repressive environment at the  
74 nuclear periphery is represented by nuclear pore complexes, where chromatin-facing  
75 nucleoporins have been implicated in transcriptional activation rather than repression in yeast  
76 (8). However, in *Drosophila*, nucleoporins appear to have this activating effect mainly in the  
77 nuclear interior (9–11). In line with the general notion that the nuclear periphery acts as a  
78 repressive environment, some though not all individual genomic loci have been shown to  
79 become transcriptionally repressed after artificial targeting to the nuclear lamina (12–16).  
80 These findings suggest a role for subnuclear position in gene regulation, however, the extent  
81 and importance of non-random localisation is poorly understood.

82

83 The *Dlk1-Dio3* imprinted domain on mouse chromosome 12 is well characterized and is a  
84 valuable model for comparative analysis of gene regulatory mechanisms. Imprinted genomic  
85 regions contain genes that are preferentially expressed from either the maternally or  
86 paternally inherited chromosome, but that also are subject to the same regulated and  
87 stochastic transcriptional mechanisms that govern the expression of other genes. Imprinted  
88 genes are therefore regulated by both germline-derived parental-origin-specific epigenetic  
89 mechanisms and the transcriptional milieu of a particular cell type (17,18). *Dlk1-Dio3*  
90 imprinting (Fig 1A) is regulated by an intergenic differentially methylated region (IGDMR)  
91 and contains a number of paternally expressed protein-coding genes as well as maternally  
92 expressed non-coding RNAs. Recent evidence has explored the relationship between the  
93 parental origin of this imprinted domain and its subnuclear locations. Kota and colleagues  
94 identified a differential localisation of the *Gtl2/Meg3* gene in a mouse embryonal stem (ES)  
95 cell line with the non-expressed paternal copy being closer to the nuclear periphery than the  
96 expressed maternal allele (19). Furthermore, a LINE1 (L1) repeat cluster located between  
97 *Begain* and *Dlk1* within the cluster (Fig.1A) was described to represent a facultative LAD in  
98 mouse ES cell-derived neural stem cells (20,21). Although this suggests that the L1 repeat  
99 might have an inhibiting effect on local gene expression via lamina tethering, deletion of the  
100 repeat cluster itself did not lead to increased expression of neighbouring genes (20). Here, we  
101 use extensive 3D RNA-DNA fluorescence-in-situ-hybridisation (FISH) in multiple normal  
102 and mutant mouse ES cell lines and show that gene expression rather than the parental origin  
103 of alleles is associated with differences in intranuclear localisation, and suggest that  
104 juxtaposition to the nuclear envelope appears to play a minor role, if any, in gene regulation  
105 at this endogenous locus.

106

107

## 108 **Results**

### 109 **Differential intranuclear distribution of parental alleles of the *Dlk1-Dio3* region.**

110

111 In order to analyse the intranuclear localisation of alleles of the *Dlk1-Dio3* region, while  
112 knowing their parental origin, we generated ES cells derived from *del*<sup>L1rep</sup> maternal and  
113 paternal heterozygous mice (20). We used only male ES cell lines for this study since it has  
114 been previously shown that imprinting status is more stable in male ES cells compared to  
115 female ES cells (22). These cells carry a deletion between the genes *Begain* and *Dlk1*, which  
116 includes a 170kb L1 repeat array (Fig. 1A and Supplementary Fig. S1) and have a normal  
117 epigenotype. Using a DNA FISH probe specific to the L1 repeat array, we used the deletion  
118 to distinguish the two parental chromosomes in 3D DNA FISH experiments, independent of  
119 gene expression. Importantly, we only quantified the behaviour of WT chromosomes not  
120 carrying the deletion. For each cell we measured the 3D distance of the DNA FISH probe to  
121 the nuclear periphery defined by the edge of DAPI staining of chromatin in an automated  
122 way (Fig. 1C). This measurement was used as a read-out for the intranuclear position of the  
123 *Dlk-Dio3* imprinted region, which lies within a single TAD in ES cells (Supplementary Fig.  
124 S1) (23,24). In parallel, we used nascent RNA FISH to obtain the *Gtl2/Meg3* expression state  
125 (expressed or non-expressed) for each allele.

126

127 We took DNA FISH probe distance measurements in three biological replicates each of  
128 heterozygous ES cells derived from maternal inheritance of *del*<sup>L1rep</sup> (matrepKO) and paternal  
129 inheritance of *del*<sup>L1rep</sup> (patrepKO) and WT ES cells, this way comparing paternally inherited  
130 alleles, maternally inherited alleles and the mixture of both as a control. Using a multiple  
131 least-squares linear regression model, we find that paternal alleles are closer to the nuclear  
132 periphery compared to maternal alleles after controlling for nuclear volume ( $t=2.946$ ,  
133  $p=0.00334$ , estimate (slope) = 0.22; Fig. 2A). Given that WT cells contained both alleles, we  
134 decided to characterise the relationship between the two alleles to understand their natural  
135 distribution within these cells. In WT cells, one allele was always closer to the nuclear border  
136 than the other, and there was a significant difference between the two alleles ( $t=22.80$ ,  
137  $p<0.001$ , estimate (slope)=1.08; Fig. 2A). While the parental origin of the WT alleles was  
138 unknown, we assume that this difference might, at least in part, reflect the tendency for the  
139 paternal allele to be biased towards the periphery. However, in the KO cells, the average  
140 difference in distance between the maternal ( $M=1.81$ ,  $SD=1.00$ ) and the paternal allele  
141 ( $M=1.58$ ,  $SD=0.954$ ) was unexpectedly small (230nm on average). Previous work had found  
142 differences of more than a micrometer, a difference that is more similar to that between the  
143 WT near and far alleles (Fig. 2A) (19). This small difference in KO was not due to variability  
144 in replicates as replicates were not significantly different from one another (Supplementary  
145 Fig. S2), but suggested that the parental origin effect we observed might be of limited  
146 functional significance. We, therefore, developed a genetic approach to compare the two  
147 parental chromosomes in a more functional context.

148

### 149 **Epigenotype switching shifts localisation**

150

151 To address the relationship between parent of origin and function more overtly we utilized  
152 genetic models exhibiting an epigenotype switch that reversed the imprints on either the  
153 maternal or the paternal chromosome. *Zfp57*KO ES cells carry a null mutation in the  
154 chromatin modifier *ZFP57*, which is important for imprint maintenance and, in case of the  
155 *Dlk1-Dio3* region, results in a paternal to maternal epigenotype switch causing a maternal

156 expression pattern from the paternally inherited chromosome (Fig. 1A and B and  
157 Supplementary Fig. S3) (25,26). Conversely, matIGDMRKO ES cells are derived from  
158 blastocysts that have a maternally inherited deletion of the IGDMR, resulting in a maternal to  
159 paternal epigenotype switch and expression of the paternally expressed imprinted genes from  
160 the maternally inherited chromosome (27). Matched WT control ES cells (WT2) were  
161 generated for this experiment. Using three biological replicates for each mutant and control  
162 line, we found that there was no significant difference in the subnuclear localisation of  
163 mutant chromosomes compared to WT between cell types ( $t=0.143$ ,  $p=n.s$ ; Fig 2B). Effects  
164 of nuclear volume were taken into account. These findings indicate that maternalising the  
165 paternal domain and paternalising the maternal domain, do not result in the expected shift in  
166 localisation. The discordance between of the findings in Figure 2A and Figure 2B  
167 experiments suggests that the epigenotype switch in the two imprinting models is not  
168 reflecting the parental origin of wildtype chromosomes in terms of subnuclear location.  
169 However, these data do not consider the transcription of imprinted loci in these models.  
170

### 171 **Stochastic or developmental repression of the maternally expressed *Gtl2/Meg3* gene** 172 **correlates with a shift of alleles towards the nuclear periphery in ES cells**

173 While *Dlk1* is not expressed in ES cells, *Gtl2/Meg3* is strongly expressed. Though all  
174 maternally inherited alleles of the *Gtl2/Meg3* gene have the potential to express the gene, it is  
175 not active in all cells. It is not known whether this effect is stochastic or regulated. Gene  
176 expression can be fine-tuned by transcription on-off cycles, sometimes called “bursting”,  
177 which could reflect genes moving in and out of transcription factories (3). Furthermore, even  
178 in the pluripotent state, some ES cells will start to differentiate, with concurrent changes in  
179 gene expression, and eventually will stop dividing in ES culture conditions. Since we cannot  
180 distinguish these possibilities in our experiments, we refer to *Gtl2/Meg3*-non-expressing  
181 maternal alleles as “stochastic or developmental repression”. Stochastic or developmental  
182 repression of the canonically active maternal allele of *Gtl2/Meg3* was observed in 29.5% of  
183 WT ES cells and 32.3% of patRepKO ES cells (Supplementary Fig. S4). We took advantage  
184 of this property to test whether active and repressed *Gtl2/Meg3* alleles differed in their  
185 intranuclear localisation using RNA FISH. We used a logistic regression approach to test if  
186 distance to the periphery predicted the expression state of *Gtl2/Meg3* (after controlling for  
187 nuclear volume variation). In three biological replicates each of patrepKO ES cell lines in  
188 which the single maternally inherited *Meg3* allele has the potential to be either expressed or  
189 not, we found no difference in localisation regardless of the expression of *Gtl2/Meg3*  
190 ( $z=1.059$ ,  $p=n.s$ ; Fig. 3A).

191 However, since *Zfp57*KO ES cells have twice as many maternal(ized) alleles as  
192 patrepKO ES cells, we reasoned that experiments with these cell lines would have greater  
193 power to examine the relationship between distance and expression. Using the same  
194 statistical methodology and same numbers of replicates, we found a non-significant trend  
195 (estimate =0.927,  $p=0.0721$ , Fig. 3B) with non-expressed alleles being marginally closer to  
196 the periphery compared to expressed alleles. As before, nuclear volume was taken into  
197 account. Together these findings indicate insignificant effects of repression on localisation  
198 relative to the nuclear periphery. We therefore focused on expressed alleles to consider  
199 whether the expression rather than repression might predict localisation.  
200

### 201 **Gene expression predicts localisation better than parental epigenotype**

202 Using *Zfp57*KO, we can measure whether biallelic expression could predict distance  
203 from the nuclear border better than monoallelic expression. Using a multiple linear mixed  
204 model approach we find that there is a marginal increase in distance when only one allele

205 within the cell is expressed ( $t=1.837$ ,  $p=0.067$ , estimate (slope) = 0.175) but alleles move  
206 significantly further from the nuclear border when both alleles are expressed ( $t=1.989$ ,  
207  $p<0.05$ , estimate (slope) =0.185; Fig 3C). This suggests that it is expression rather than  
208 parental epigenotype or repression that confers subnuclear localisation. Consistent with this  
209 and as shown in Fig 4A, expressed alleles are more likely to be greater than  $0.5\mu\text{m}$  away  
210 from the periphery ( $\chi^2=3.0713$ ,  $df=1$ ,  $p=0.08$ ). To examine this at higher resolution, we  
211 plotted the regional location after dividing the nucleus into thirds by volume (outer, middle,  
212 inner ) as has been described previously (19). Results suggest that repressed alleles are not  
213 preferentially located to the periphery, rather, active alleles are enriched away from the  
214 periphery ( $\chi^2=14.206$ ,  $df=2$ ,  $p<0.001$ ; Fig 4B).

215

## 216 Discussion

217

218 We performed 3D RNA-DNA FISH measurements in a total of 18 mouse ES cell  
219 lines and observed a very small but overall highly significant effect for *Gtl2/Meg3*-expressing  
220 alleles of the *Dlk1-Dio3* imprinted region to be localized towards the nuclear interior and for  
221 non-expressing alleles to be localized towards the nuclear periphery. As has been shown  
222 before (19), paternal alleles, which do not express *Gtl2/Meg3*, localize overall closer to the  
223 periphery than maternal alleles, from which *Gtl2/Meg3* is expressed in 70.5% of WT ES  
224 cells. Differences in localisation between paternalized and maternalized alleles (i.e.,  
225 IGDMRKO vs ZFP57KO) are only evident when expression state is considered. In other  
226 words, expressed *Gtl2/Meg3* alleles are positioned further away from the periphery than non-  
227 expressed alleles. Furthermore, the position within the nucleus is directly related to the  
228 number of alleles being expressed within a given cell, as evident through the analysis of cells  
229 expressing zero, one or two alleles.

230 The effect size of the localisation difference between expressing and non-expressing  
231 alleles in our study is much smaller than that previously described (19). Three notable  
232 differences between our work and the previous study might explain this: 1) Kota et al. used  
233 *Gtl2/Meg3* expression as a read-out for parental origin while we included an independent  
234 DNA marker and genetic approaches allowing us to distinguish and quantify expressing and  
235 non-expressing maternal chromosomes. 2) Kota et al. used one biological replicate hence  
236 would not have been able to take into account the variability that is evident between lines. 3)  
237 Our edge measurements utilise a DNA marker located 400kb away from the interrogated  
238 gene which might result in lower data resolution (supplementary Fig. S1). Both genetic  
239 locations lie, however, within the same TAD in ES cells (23,24) and show frequent overlap in  
240 a double probe DNA FISH experiment using probes against the L1 repeat and the *Gtl2/Meg3*  
241 gene (Supplementary Fig. S1 and S5). Our findings reflect the importance of independently  
242 distinguishing parental chromosomes and expression and then determining the contribution  
243 that each makes to subnuclear localisation.

244 Mouse ES cells show an unusual cell cycle distribution where a majority of cells  
245 (75%) will be in S-phase in a growing cell population (28). S-phase can potentially have an  
246 influence on gene expression and cell cycle heterogeneity could thus be a source of  
247 variability between biological replicates. However, when comparing nuclear sizes (as a proxy  
248 for cell-cycle differences) of expressing and non-expressing alleles as well as biological  
249 replicates, some small variation in nuclear size was evident in some instances  
250 (Supplementary Fig. S6). We therefore included nuclear volume as a covariate in all of our  
251 analyses to correct for any minor fluctuations in nuclear volume. Hence, all of our estimates  
252 of the differences in allelic distribution control for minor changes in nuclear volume.

253 Though data from all our ES cell lines show a significant expression-dependent effect  
254 on subnuclear localisation, the effect size is extremely small with *Gtl2/Meg3*-non-expressing

255 alleles being on average only 170 nm closer to the nuclear periphery than *Gtl2/Meg3*-  
256 expressing alleles. Indeed, most expressed alleles can be more broadly categorised as being  
257 away from the periphery (or outer most region) though not extremely central to the nucleus. It  
258 is interesting to consider whether such a small effect is biologically meaningful. Since we did  
259 not observe a significant enrichment of inactive alleles in the immediate vicinity of the  
260 nuclear envelope, inactivating interactions with the nuclear lamina are unlikely to play a  
261 major role in the observed allele distribution. Notably, *Gtl2/Meg3* expression was regularly  
262 found right at the edge of DAPI staining and occasionally outside of it, probably representing  
263 areas of low density chromatin at the very periphery of nuclei (see methods section for  
264 details). Although it can be envisioned that in some cases *Gtl2/Meg3* expression might have  
265 been inhibited by transient nuclear envelope interactions and had already moved away from  
266 the periphery at the time of the experiment, such alleles should still show up as peripheral  
267 enrichment since mobility of individual loci during interphase is usually limited to about 1  
268  $\mu\text{m}$  and it has been shown that large scale changes in localization require cell division (1,29).  
269 A more likely explanation is that the observed pattern of allele localisation is due to some  
270 activating effect of structures at the nuclear interior. This is consistent with the increase in  
271 internalisation observed when two alleles are expressed compared to one in a given cell.  
272 Transcription is known to happen preferentially at sites where the transcriptional machinery  
273 and active genes are clustered into so-called transcription factories (3,4). Such factories are  
274 found in open chromatin at the borders of chromosomal territories and it seems logical that  
275 they would be biased to be more frequent at the more transcriptionally favourable nuclear  
276 interior. Therefore, one possible explanation for the observed non-enrichment at the nuclear  
277 periphery and the small effect size of our expression-localisation correlation could be that  
278 *Gtl2/Meg3*-non-expressing alleles are evenly distributed within the space they can take up  
279 around the chromosome territory, independent of nuclear envelope interactions, while  
280 *Gtl2/Meg3*-expressing alleles need to be localized at transcription factories which are biased  
281 to be at the interior. It would be interesting to test this idea by co-localising expressing and  
282 non-expressing alleles with components of transcriptional factories. Nevertheless, our use of  
283 multiple biological replicates in multiple genetic models highlights the wide range of  
284 positions that an allele can take within the nucleus regardless of expression status.

285 For all correlations of nuclear localisation and expression, the question of cause and  
286 consequence arises. Is peripheral localisation used as a means to fine-tune gene expression by  
287 making the co-localisation with transcription factories more or less likely? The absence of  
288 enrichment of inactive alleles at the nuclear periphery does not argue for such a mechanism.  
289 Kota and colleagues have shown that position changes of the *Dlk1-Dio3* region are local and  
290 do not involve gross changes in chromosome territory (19). Similarly, our *Zfp57* mutants  
291 show that local and purely epigenetic changes are sufficient to cause a shift in localisation at  
292 the same time as inducing *Gtl2/Meg3* gene expression. This argues that a nuclear envelope  
293 anchoring mechanism acting at a distance is unlikely to be involved. A local anchoring  
294 mechanism on the other hand should show up as peripheral enrichment which we do not  
295 observe. We therefore suggest that the small shift in peripheral localisation that we observe is  
296 a consequence, rather than a cause of expression changes and that the more functionally  
297 relevant aspect is the interior location of expressed alleles which is influenced by the number  
298 of alleles being expressed.

299  
300

## 301 **Methods**

302

### 303 **Cell culture**



304 Mutant and corresponding control ES cells were generated from single blastocyst using  
305 feeder-free-based 2i LIF culture conditions (N2B27, Stem Cell Sciences) (30). In brief,  
306 morula embryos were collected from pregnant female mice and cultured in KSOM with 2i  
307 inhibitors, and then each blastocyst was genotyped using trophectoderm after  
308 immunosurgery. *deJ*<sup>L1rep</sup> mice have an *albino* C57BL/6J background (BL6) (20) and were  
309 crossed to *albino* BL6 mice to obtain WT, maternal and paternal heterozygotes. IG-DMR  
310 heterozygous females (27) were mated with BL6 males to obtain IG-DMR maternal KO and  
311 control WT morula embryos. *Zfp57* zygotic KO ES cells and corresponding control ES cells  
312 were generated in a previous study (26). The research was conducted in accordance with UK  
313 Home Office Animals Scientific Procedures Act, project licence 80/2567. We observed  
314 unexpectedly low expression levels of *Gtl2/Meg3* in two of five *Zfp57*KOES cell lines and  
315 therefore excluded these two cell lines from these studies. For our analysis of ES cells of all  
316 genotypes, we used data from the three biological replicates that showed the expected and  
317 similar proportions of non-expressing, monoallelically expressing, and biallelically  
318 expressing cells (Supplementary Fig. S2).  
319

### 320 **Fluorescence in situ hybridisation**

321 We generated fluorescent probes for detection of the LINE repeat (BAC bMQ-177C10,  
322 obtained from CHORI) and nascent *Gtl2/Meg3* transcripts (fosmid WIBR1-2686H19, a kind  
323 gift from the Heard lab, Paris) by first amplifying plasmid mini preps with the Illustra  
324 TempliPhi Large Construct Kit (GE Healthcare) and subsequently labelling 2 µg of the  
325 amplification product by nick translation using Green UTP or Red UTP (Abbott Molecular)  
326 according to the manufacturer's instructions. Sequential RNA and DNA 3D fluorescence in  
327 situ hybridisation (FISH) was performed as previously described (31). However, ES cells  
328 were grown on laminin-coated coverslips prior to fixing to ensure well-spread monolayer  
329 growth and nuclei were counterstained with 0.2 µg/ml DAPI after hybridisation and washes.  
330 3D image stacks of 10-15 positions per coverslip were acquired using a Carl Zeiss Axiovert  
331 200M microscope with a 63x/1.25 Plan Apochromat objective taking 100 image planes per  
332 image stack at a z spacing of 0.15 µm. For double probe DNA FISH the same protocol was  
333 used as in sequential FISH and the *Gtl2/Meg3* fosmid probe was used to detect the gene  
334 rather than nascent RNA.  
335

### 336 **Image analysis**

337 DNA FISH image stacks were post-processed using Huygens Professional deconvolution  
338 software (version 14.10.1p8, SVI, The Netherlands) and 3D measurements were taken using  
339 Fiji (32). We developed a Fiji script that enabled us to generate binary representations of  
340 DAPI-stained nuclei and FISH signals and to take automated 3D measurements of and  
341 between these objects calling Fiji's 3D manager function (Fig. 1C). If FISH signals were  
342 duplicated due to DNA replication, we used the mean of both measurements for the analysis.  
343 Due to the nature of the binarization process using DAPI staining of chromatin, binary  
344 images of nuclei sometimes differed slightly in shape from what was seen by eye in the  
345 original image because, depending on image background levels or closeness of neighbouring  
346 nuclei, non-dense chromatin regions were interpreted as background by the algorithm. This  
347 led to a minority of DNA FISH signals (2.8%) being outside the nuclear volume. To avoid  
348 bias against peripherally located signals, we included such signals as negative distance  
349 measurements. In very rare cases the algorithm generated a bay-like background area around  
350 a FISH signal in a non-dense chromatin area, in a way that our standard automated  
351 measurements would lead to false results. Again, to avoid biasing against peripheral signals  
352 as well as inaccurate manual measuring, in these rare cases (0.3%) we used an alternative

353 algorithm that approximates the nuclear volume by fitting an ellipse around the original shape  
354 and used this shape for distance measurements. For relative distance measurements, we used  
355 the “radiusCen” measurement of Fiji’s 3D manager, which measured the distance between  
356 the centre of the binary representation of the nucleus and its border through the centre of the  
357 binary representation of the FISH signal, as local nuclear radius. Relative distances were  
358 calculated as absolute distance / local nuclear radius. In parallel to DNA FISH analysis, the  
359 expression state of the *Gtl2/Meg3* gene was evaluated from original (non-deconvolved)  
360 nascent RNA FISH image stacks for each allele as either expressed (FISH signal above  
361 background level) or non-expressed (no signal).

### 362 **Statistical methodology**

363 All analyses used a linear regression model framework using nuclear size as a covariate (to  
364 control for any volume effects on expression and/or localisation) using base R regression  
365 functions (33). Given that some cells had measurements for multiple alleles, where  
366 appropriate, we used mixed effects linear regression models using the lme4 and lmerTest  
367 packages in R (34,35) to allow for random intercepts (of unique cells) which effectively  
368 controls variability arising from the repeated measurement of unique cells (36). Data  
369 handling and visualisation in R was carried out using the ‘tidyverse’ packages (37). Chi-  
370 squared tests for differences in nuclear volume distributions were calculated using base chi.sq  
371 functions in R.

372

### 373 **Acknowledgements**

374 We would like to thank Richard Butler at the Gurdon Institute Imaging Facility, Cambridge,  
375 for help with writing Fiji macros for 3D image analysis, Edith Heard, Simao daRocha and  
376 Luca Giorgetti at the Institute Pierre et Marie Curie, Paris, for helpful advice with FISH  
377 methods, and David Glover and George Tzolovsky at the Department of Genetics,  
378 Cambridge, for microscopy support. This work was funded by a DFG research fellowship NE  
379 1959/1-1 to LCH and grants from the Wellcome Trust and MRC to ACFS. The authors  
380 declare no conflict of interest.

381

### 382 **Authors contributions**

383 LCH and ACFS conceived and designed the experiments. LCH and FLD conducted the FISH  
384 experiments and LCH and RM conducted the data analysis. NT generated and tested the ES  
385 cell lines. LCH, RM and ACFS wrote the paper.

386

387

388

389

390

391

392

393

## Figure legends

**Figure 1: Experimental design.** (A) A 260kb deletion encompassing the LINE1 cluster in the *Dlk1-Dio3* imprinted region was used to mark the parental origin of alleles. ES cells derived from mutant mice were used that mimic a uniparental origin of the *Dlk1-Dio3* region. ES cells with a homozygous deletion of the chromatin modifier *Zfp57* show maternal expression patterns at the paternally inherited chromosome while ES cells with a maternally inherited deletion of the IGDMR show paternal expression patterns from the maternally inherited chromosome. The FISH images of ES cells, where the maternal L1 cluster was used for 3D measurements and *Gtl2/Meg3* expression was assessed in parallel. As predicted, many *Zfp57*KO ES cells showed biallelic expression of maternally expressed *Gtl2/Meg3*, while matIGDMRKO ESC showed no *Gtl2/Meg3* expression. Chromosome maps are derived from Soares et al. 2018 (20). The FISH images represent maximum projections of 20-30 central z planes of acquired image stacks. Blow-ups of framed regions are shown on the right. Scale bars represent 50  $\mu$ m. (B) Schematic of nuclei with the expected combined DNA and RNA FISH results for all genotypes. (C) Automated, unbiased, distance measurements using the Fiji imaging package. Each nucleus is manually selected from the FISH image stack and both channels are binarized and added to Fiji's 3D manager to automatically measure the shortest distance from the centre of the FISH signal to the chromatin border in 3D. The shortest distance might be oriented more in the xy axis (i) or more in the z axis (ii) of the image stack. Occasionally, peripheral FISH signals were just outside of the chromatin representation (iii) and therefore measured as negative distances (See Methods).

**Figure 2: Distribution of alleles by parental origin.** (A) Paternal alleles (matrepKO) of the *Dlk1-Dio3* are significantly closer to the nuclear periphery than maternal alleles (patrepKO), as has been reported previously. This difference is less pronounced than the natural difference between the two alleles within a WT cell (\*\* $p < 0.01$ ). (B) There were no differences in the distance from the periphery between paternal and paternalized alleles from matIGDMRKO ES cells or maternal and maternalized alleles from *Zfp57*KO ES cells from WT cells.

**Figure 3: Distribution of alleles depending on *Gtl2/Meg3* gene expression.** (A) There was no relationship between localisation and *Gtl2/Meg3* expression from patrepKO ESCs. (B) Maternalized alleles from *Zfp57*KO ES cells were marginally closer to the edge when *Gtl2/Meg3* was non-expressed ( $\#p < 0.1$ ), (C) Maternal(ized) alleles split by number of alleles that were expressed. Alleles that were expressed alone in the cell were marginally farther from the periphery than alleles that were not expressed. However, alleles that had both alleles expressed within the cell were significantly further away from the periphery ( $\#p < 0.1$ , \* $p < 0.05$ ).

**Figure 4: *Gtl2/Meg3*-non-expressing maternal(ized) alleles are not enriched at the nuclear periphery.** (A) *Gtl2/Meg3* expressing chromosomes (patrepKO and *Zfp57*KO) alleles show a significant shift away from the nuclear periphery compared to non-expressed alleles. (B) If the allele distribution is depicted as relative to the nuclear radius, the shift is still visible with a greater proportion of *Gtl2/Meg3* expressed alleles in inner and middle areas.

## References

1. van Steensel B, Belmont AS. Lamina-Associated Domains: Links with Chromosome Architecture, Heterochromatin, and Gene Repression. Vol. 169, *Cell*. 2017.
2. Cremer T, Cremer C. Chromosome territories, nuclear architecture and gene regulation in mammalian cells. Vol. 2, *Nature Reviews Genetics*. 2001. p. 292–301.
3. Osborne CS, Chakalova L, Brown KE, Carter D, Horton A, Debrand E, et al. Active genes dynamically colocalize to shared sites of ongoing transcription. *Nature Genetics*. 2004;36(10):1065–71.
4. Nguyen HQ, Bosco G. Gene Positioning Effects on Expression in Eukaryotes. *Annual Review of Genetics*. 2015;49(1).
5. Shachar S, Misteli T. Causes and consequences of nuclear gene positioning. *Journal of Cell Science*. 2017;130(9).
6. Guelen L, Pagie L, Brasset E, Meuleman W, Faza MB, Talhout W, et al. Domain organization of human chromosomes revealed by mapping of nuclear lamina interactions. *Nature*. 2008;453(7197):948–51.
7. Kind J, Pagie L, Ortobozkoyun H, Boyle S, De Vries SS, Janssen H, et al. Single-cell dynamics of genome-nuclear lamina interactions. *Cell*. 2013;153(1):178–92.
8. Casolari JM, Brown CR, Komili S, West J, Hieronymus H, Silver PA. Genome-wide localization of the nuclear transport machinery couples transcriptional status and nuclear organization. *Cell*. 2004;117(4):427–39.
9. Kalverda B, Pickersgill H, Shloma V V., Fornerod M. Nucleoporins Directly Stimulate Expression of Developmental and Cell-Cycle Genes Inside the Nucleoplasm. *Cell*. 2010;140(3):360–71.
10. Capelson M, Liang Y, Schulte R, Mair W, Wagner U, Hetzer MW. Chromatin-Bound Nuclear Pore Components Regulate Gene Expression in Higher Eukaryotes. *Cell*. 2010;140(3):372–83.
11. Vaquerizas JM, Suyama R, Kind J, Miura K, Luscombe NM, Akhtar A. Nuclear pore proteins Nup153 and megator define transcriptionally active regions in the *Drosophila* genome. *PLoS Genetics*. 2010;6(2).
12. Finlan LE, Sproul D, Thomson I, Boyle S, Kerr E, Perry P, et al. Recruitment to the nuclear periphery can alter expression of genes in human cells. *PLoS Genetics*. 2008;4(3).
13. Reddy KL, Singh H. Using molecular tethering to analyze the role of nuclear compartmentalization in the regulation of mammalian gene activity. *Methods*. 2008;45(3):242–51.

14. Zullo JM, Demarco IA, Piqué-Regi R, Gaffney DJ, Epstein CB, Spooner CJ, et al. DNA sequence-dependent compartmentalization and silencing of chromatin at the nuclear lamina. *Cell*. 2012;149(7):1474–87.
15. Dialynas G, Speese S, Budnik V, Geyer PK, Wallrath LL. The role of *Drosophila* Lamin C in muscle function and gene expression. *Development*. 2010;137(18):3067–77.
16. Kumaran RI, Spector DL. A genetic locus targeted to the nuclear periphery in living cells maintains its transcriptional competence. *Journal of Cell Biology*. 2008;180(1):51–65.
17. Ferguson-Smith AC. Genomic imprinting: the emergence of an epigenetic paradigm. *Nature Reviews Genetics*. 2011;12(8):565–75.
18. McEwen KR, Ferguson-Smith AC. Distinguishing epigenetic marks of developmental and imprinting regulation. *Epigenetics and Chromatin*. 2010;3(1).
19. Kota SK, Llères D, Bouchet T, Hirasawa R, Marchand A, Begon-Pescia C, et al. ICR noncoding RNA expression controls imprinting and DNA replication at the *Dlk1-Dio3* domain. *Developmental Cell*. 2014;31(1):19–33.
20. Soares ML, Edwards CA, Dearden FL, Ferron SR, Curran S, Corish J, et al. Targeted deletion of a 170 kb cluster of LINE1 repeats: implications for regional control. *Genome research*. 2018;gr.221366.117.
21. Peric-Hupkes D, Meuleman W, Pagie L, Bruggeman SWM, Solovei I, Brugman W, et al. Molecular Maps of the Reorganization of Genome-Nuclear Lamina Interactions during Differentiation. *Molecular Cell*. 2010;38(4):603–13.
22. Sun B, Ito M, Mendjan S, Ito Y, Brons IGM, Murrell A, et al. Status of genomic imprinting in epigenetically distinct pluripotent stem cells. *Stem Cells*. 2012;30(2):161–8.
23. Schoenfelder S, Furlan-Magaril M, Mifsud B, Tavares-Cadete F, Sugar R, Javierre BM, et al. The pluripotent regulatory circuitry connecting promoters to their long-range interacting elements. *Genome Research*. 2015;
24. Dixon JR, Selvaraj S, Yue F, Kim A, Li Y, Shen Y, et al. Topological domains in mammalian genomes identified by analysis of chromatin interactions. *Nature*. 2012;485(7398):376–80.
25. Li X, Ito M, Zhou F, Youngson N, Zuo X, Leder P, et al. A Maternal-Zygotic Effect Gene, *Zfp57*, Maintains Both Maternal and Paternal Imprints. *Developmental Cell*. 2008;15(4):547–57.
26. Shi H, Strogantsev R, Takahashi N, Kazachenka A, Lorincz MC, Hemberger M, et al. *ZFP57* regulation of transposable elements and gene expression within and beyond imprinted domains. *Epigenetics Chromatin*. 2019 Aug 9;12(1):49.
27. Lin SP, Youngson N, Takada S, Seitz H, Reik W, Paulsen M, et al. Asymmetric regulation of imprinting on the maternal and paternal chromosomes at the *Dlk1-Gtl2* imprinted cluster on mouse chromosome 12. *Nature Genetics*. 2003;35(1):97–102.

28. Savatier P, Lapillonne H, Jirmanova L, Vitelli L, Samarut J. Analysis of the Cell Cycle in Mouse Embryonic Stem Cells. *Embryonic Stem Cells*. 185(3):27–33.
29. Kind J, Pagie L, De Vries SS, Nahidiazar L, Dey SS, Bienko M, et al. Genome-wide Maps of Nuclear Lamina Interactions in Single Human Cells. *Cell*. 2015;163(1).
30. Ying Q-L, Ying Q-L, Wray J, Wray J, Nichols J, Nichols J, et al. The ground state of embryonic stem cell self-renewal. *Nature*. 2008;453(May):519–23.
31. Giorgetti L, Galupa R, Nora EP, Piolot T, Lam F, Dekker J, et al. Predictive polymer modeling reveals coupled fluctuations in chromosome conformation and transcription. *Cell*. 2014;157(4):950–63.
32. Schindelin J, Arganda-Carreras I, Frise E, Kaynig V, Longair M, Pietzsch T, et al. Fiji: an open-source platform for biological-image analysis. *Nature Methods*. 2012;9(7):676–82.
33. R Core Team. R: A Language and Environment for Statistical Computing [Internet]. Vienna, Austria: R Foundation for Statistical Computing; 2019. Available from: <https://www.R-project.org/>
34. Bates D, Mächler M, Bolker B, Walker S. Fitting Linear Mixed-Effects Models Using **lme4**. *J Stat Soft* [Internet]. 2015 [cited 2020 Jan 3];67(1). Available from: <http://www.jstatsoft.org/v67/i01/>
35. Kuznetsova A, Brockhoff PB, Christensen RHB. lmerTest Package: Tests in Linear Mixed Effects Models. *J Stat Soft* [Internet]. 2017 [cited 2020 Jan 3];82(13). Available from: <http://www.jstatsoft.org/v82/i13/>
36. Gelman A, Hill J. *Data Analysis Using Regression and Multilevel/Hierarchical Models* [Internet]. Cambridge: Cambridge University Press; 2006 [cited 2020 Jan 3]. Available from: <http://ebooks.cambridge.org/ref/id/CBO9780511790942>
37. Wickham H, Averick M, Bryan J, Chang W, McGowan L, François R, et al. Welcome to the Tidyverse. *JOSS*. 2019 Nov 21;4(43):1686.

## Supplementary Information

**Supplementary Figure S1:** UCSC (<https://genome.ucsc.edu/>) -screenshot of the Dlk1-Dio3 imprinted region in mouse mm9 showing the exact positions of RNA (Meg3) and DNA (L1 repeat) FISH probes, as well as the genomic distances between them (inner, central and outer distance). The exact position of the LINE1 repeat deletion (20) in relation to the repeat probe and the UCSC RepeatMasker are also shown. The top panel shows ES cell TADs from Schoenfelder and colleagues (Bab\_ESC) and Dixon and colleagues (Ren\_ESC) loaded as custom tracks (23,24)

**Supplementary Figure S2:** Plots of the distance from the nuclear border relative to *Gtl2/Meg3* expression in individual biological replicates of all KO and WT groups measured in the study. We find no significant effect of replicate on overall distance measures.

**Supplementary Figure S3:** Additional examples of gene expression in the five ES cells genotypes at larger magnifications (compare figure 1). *Gtl2/Meg3* probe stained images are from nascent RNA FISH and L1 Repeat probe stained images are from subsequent DNA FISH. The FISH images represent maximum projections of 10-30 central z planes of acquired image stacks. Blow-ups of framed regions are shown on the right. Scale bars represent 50  $\mu\text{m}$ .

**Supplementary Figure S4:** Numbers of cells per cell line with no, monoallelic, or biallelic *Gtl2/Meg3* expression.

**Supplementary Figure S5:** Double probe DNA FISH in WT ES cells (ES cell line WT8). The images show only one z image plane. All three locations, at which the L1 repeat signal and the *Gtl2/Meg2* gene signal have their centres roughly in the same z image plane, are shown as blow-ups on the right. The distance between the signal centres is between 0.25 and 0.36  $\mu\text{m}$  in these three examples.

**Supplementary Figure S6:** The density of nuclear sizes does not vary considerably between *Gtl2/Meg3*-expressing and -non-expressing ES cells and therefore does not hint towards a specific down- or upregulation of gene activity during s-phase.

**Supplementary Table 1:** CSV file of raw data and metadata from all experimental cell lines.

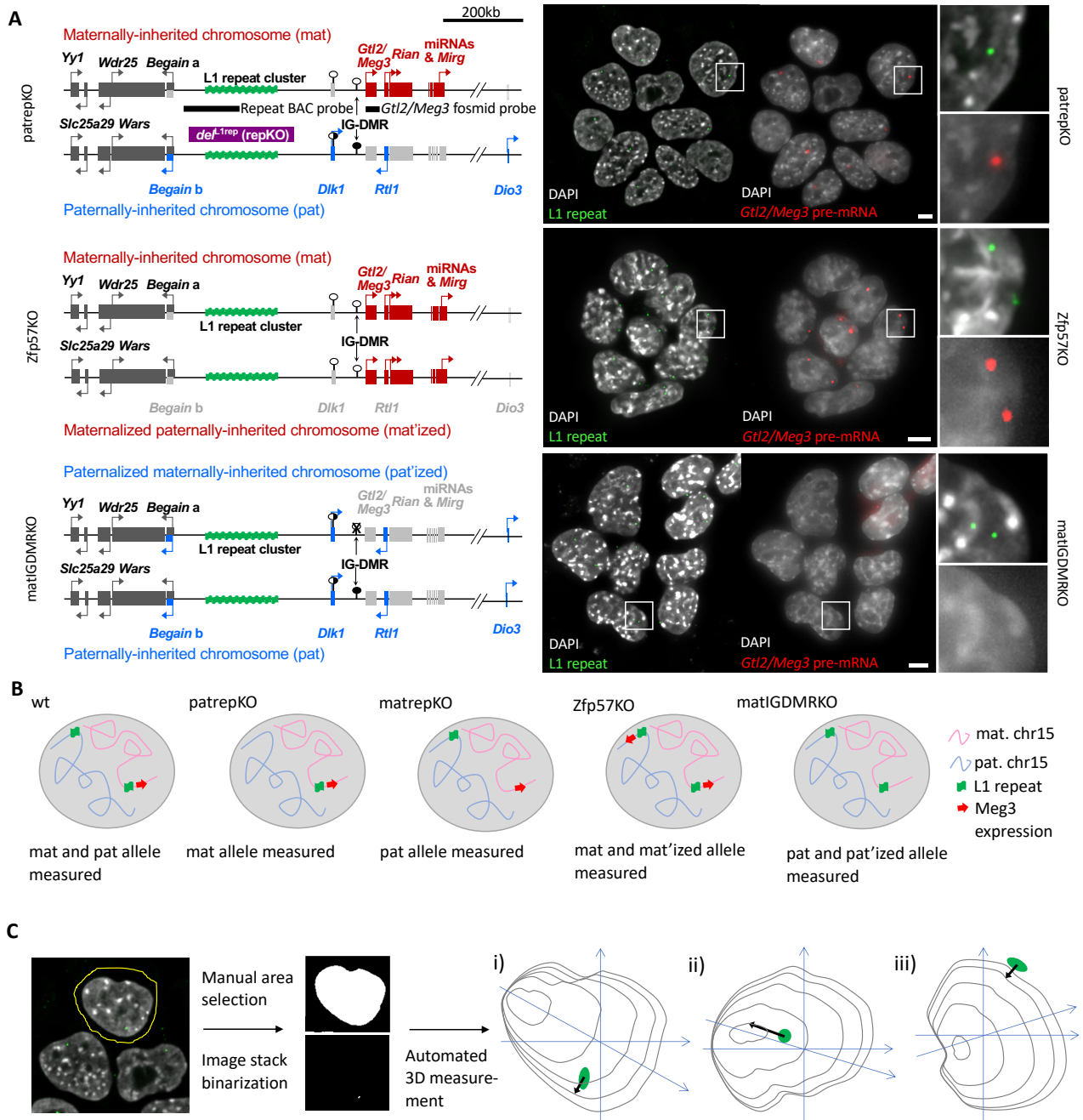




**Figure 2**

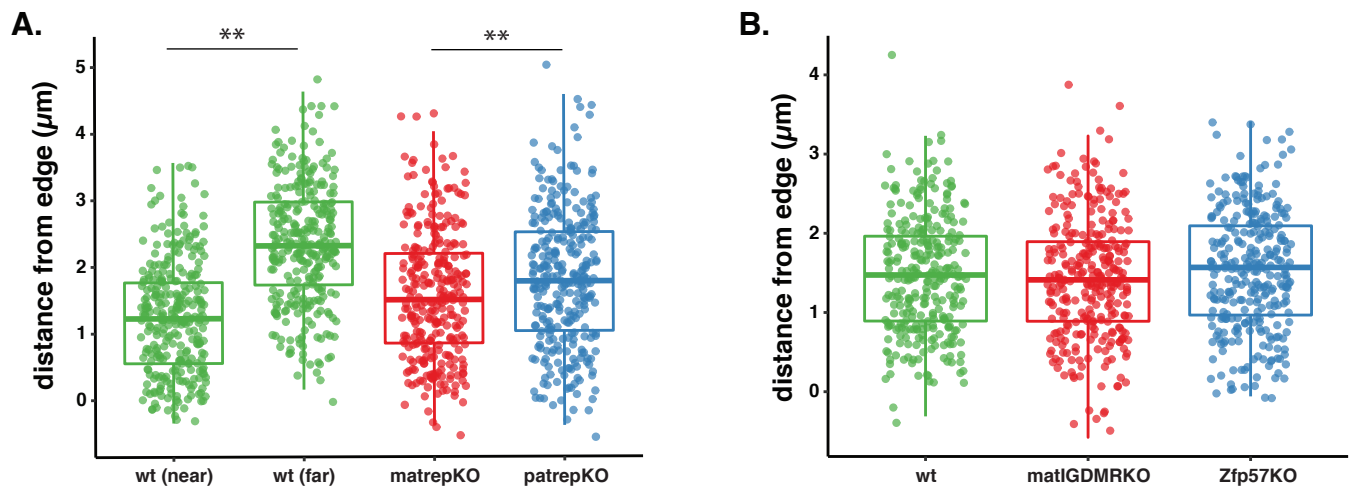


Figure 3

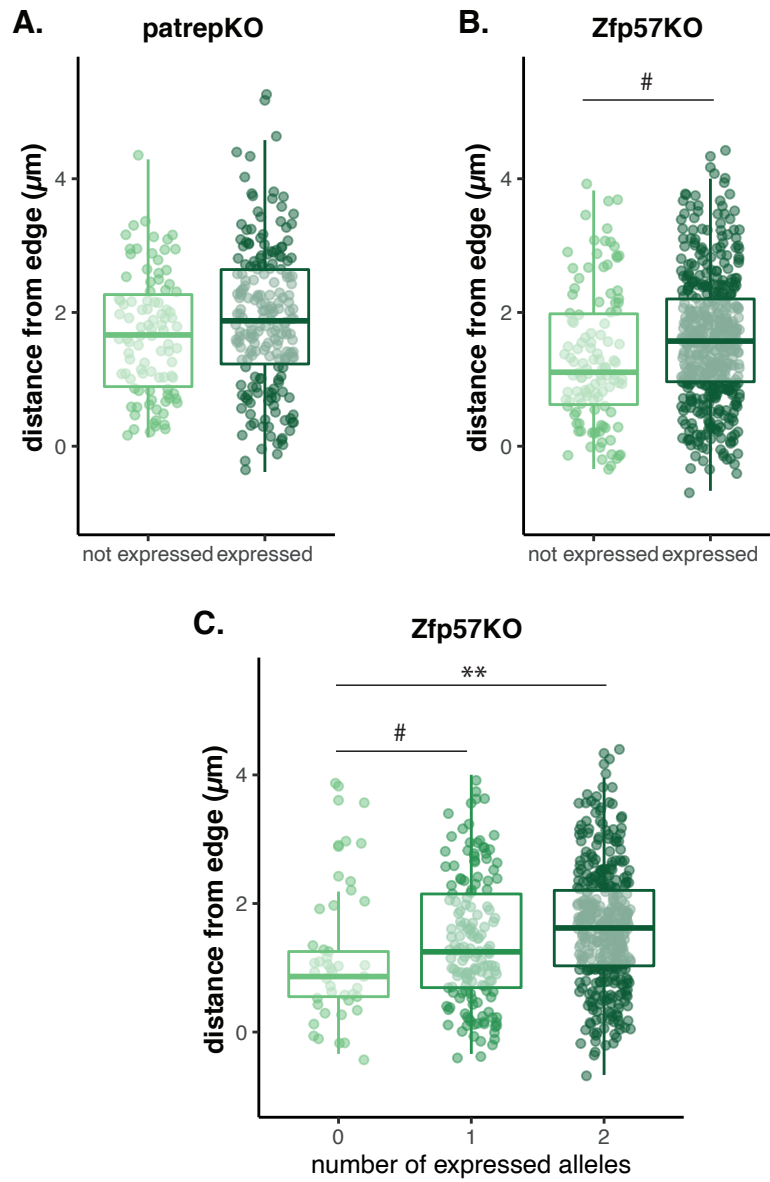


Figure 4

